Measurement of the neutrino velocity with the OPERA detector in the CNGS beam

T. Adam[a], N. Agafonova[b], A. Aleksandrov[c,1], O. Altinok[d], P. Alvarez Sanchez[e], S. Aoki[f], A. Ariga[g], T. Ariga[g], D. Autiero[h], A. Badertscher[i], A. Ben Dhahbi[g], A. Bertolin[j], C. Bozza[k], T. Brugière[h], F. Brunet[l], G. Brunetti[h,m,2], S. Buontempo[c], F. Cavanna[n], A. Cazes[h], L. Chaussard[h], M. Chernyavskiy[o], V. Chiarella[p], A. Chukanov[q], G. Colosimo[r], M. Crespi[r], N. D'Ambrosio[s], Y. Déclais[h], P. del Amo Sanchez[l], G. De Lellis[t,c], M. De Serio[u], F. Di Capua[c], F. Cavanna[p], A. Di Crescenzo[t,c], D. Di Ferdinando[v], N. Di Marco[s], S. Dmitrievsky[q], M. Dracos[a], D. Duchesneau[l], S. Dusini[j], J. Ebert[w], I. Eftimiopolous[e], O. Egorov[x], A. Ereditato[g], L.S. Esposito[i], J. Favier[l], T. Ferber[w], R.A. Fini[u], T. Fukuda[y], A. Garfagnini[z,j], G. Giacomelli[m,v], C. Girerd[h], M. Giorgini[m,v,3], M. Giovannozzi[e], J. Goldberg[aa], C. Göllnitz[w], L. Goncharova[o], Y. Gornushkin[q], G. Grella[k], F. Grianti[ab,p], E. Gschewentner[e], C. Guerin[h], A.M. Guler[d], C. Gustavino[ac], K. Hamada[ad], T. Hara[f], M. Hierholzer[w], A. Hollnagel[w], M. Ieva[u], H. Ishida[y], K. Ishiguro[ad], K. Jakovcic[ae], C. Jollet[a], M. Jones[e], F. Juget[g], M. Kamiscioglu[d], J. Kawada[g], S.H. Kim[af,4], M. Kimura[y], N. Kitagawa[ad], B. Klicek[ae], J. Knuesel[g], K. Kodama[ag], M. Komatsu[ad], U. Kose[j], I. Kreslo[g], C. Lazzaro[i], J. Lenkeit[w], A. Ljubicic[ae], A. Longhin[p], A. Malgin[b], G. Mandrioli[v], J. Marteau[h], T. Matsuo[y], N. Mauri[p], A. Mazzoni[r], E. Medinaceli[z,j], F. Meisel[g], A. Meregaglia[a], P. Migliozzi[c], S. Mikado[y], D. Missiaen[e], K. Morishima[ad], U. Moser[g], M.T. Muciaccia[ah,u], N. Naganawa[ad], T. Naka[ad], M. Nakamura[ad], T. Nakano[ad], Y. Nakatsuka[ad], D. Naumov[q], V. Nikitina[ai], S. Ogawa[y], N. Okateva[o], A. Olchevsky[s], O. Palamara[s], A. Paoloni[p], B.D. Park[af,5], I.G. Park[af], A. Pastore[ag,u], L. Patrizii[v], E. Pennacchio[h], H. Pessard[l], C. Pistillo[g], N. Polukhina[o], M. Pozzato[m,v], K. Pretzl[g], F. Pupilli[s], R. Rescigno[k], T. Roganova[ai], H. Rokujo[f], G. Rosa[aj,ac], I. Rostovtseva[x], A. Rubbia[i], A. Russo[c], O. Sato[ad], Y. Sato[ak], A. Schembri[s], J. Schuler[a], L. Scotto Lavina[g,6], J. Serrano[e], A. Sheshukov[q], H. Shibuya[y], G. Shoziyoev[ai], S. Simone[ah,u], M. Sioli[m,v], C. Sirignano[s], G. Sirri[v], J.S. Song[af], M. Spinetti[p], N. Starkov[o], M. Stellacci[k], M. Stipcevic[ae], T. Strauss[g], P. Strolin[t,c], S. Takahashi[f], M. Tenti[m,v,h], F. Terranova[p], I. Tezuka[ak], V. Tioukov[c], P. Tolun[d], T. Tran[h], S. Tufanli[g], P. Vilain[al], M. Vladimirov[o], L. Votano[p], J.-L. Vuilleumier[g], G. Wilquet[al], B. Wonsak[w], J. Wurtz[a], C.S. Yoon[af], J. Yoshida[ad], Y. Zaitsev[x], S. Zemskova[q], A. Zghiche[l]

1 On leave of absence from LPI-Lebedev Physical Institute of the Russian Academy of Sciences, 119991 Moscow, Russia
2 Now at Albert Einstein Center for Fundamental Physics, Laboratory for High Energy Physics (LHEP), University of Bern, CH-3012 Bern, Switzerland
3 Now at INAF/IASF, Sezione di Milano, I-20133 Milano, Italy
4 Now at Pusan National University, Geumjeong-Gu, Busan 609-735, Republic of Korea
5 Now at Asian Medical Center, 388-1 Pungnap-2 Dong, Songpa-Gu, Seoul 138-736, Republic of Korea
6 Now at SUBATECH, CNRS/IN2P3, F-44307 Nantes, France
a IPHC, Université de Strasbourg, CNRS/IN2P3, F-67037 Strasbourg, France
b INR-Institute for Nuclear Research of the Russian Academy of Sciences, RUS-327312 Moscow, Russia
c INFN Sezione di Napoli, I-80125 Napoli, Italy
d METU-Middle East Technical University, TR-06532 Ankara, Turkey
e European Organization for Nuclear Research (CERN), Geneva, Switzerland
f Kobe University, J-657-8501 Kobe, Japan

[g] Albert Einstein Center for Fundamental Physics, Laboratory for High Energy Physics (LHEP), University of Bern, CH-3012 Bern, Switzerland

[h] IPNL, Université Claude Bernard Lyon I, CNRS/IN2P3, F-69622 Villeurbanne, France

[i] ETH Zurich, Institute for Particle Physics, CH-8093 Zurich, Switzerland

[j] INFN Sezione di Padova, I-35131 Padova, Italy

[k] Dipartimento di Fisica dell'Università di Salerno and INFN "Gruppo Collegato di Salerno", I-84084 Fisciano, Salerno, Italy

[l] LAPP, Université de Savoie, CNRS/IN2P3, F-74941 Annecy-le-Vieux, France

[m] Dipartimento di Fisica dell'Università di Bologna, I-40127 Bologna, Italy

[n] Dipartimento di Fisica dell'Università dell'Aquila and INFN "Gruppo Collegato de L'Aquila", I-67100 L'Aquila, Italy

[o] LPI-Lebedev Physical Institute of the Russian Academy of Science, RUS-119991 Moscow, Russia

[p] INFN - Laboratori Nazionali di Frascati, I-00044 Frascati (Roma), Italy

[q] JINR-Joint Institute for Nuclear Research, RUS-141980 Dubna, Russia

[r] Area di Geodesia e Geomatica, Dipartimento di Ingegneria Civile Edile e Ambientale dell'Università di Roma Sapienza, I-00185 Roma, Italy

[s] INFN - Laboratori Nazionali del Gran Sasso, I-67010 Assergi (L'Aquila), Italy

[t] Dipartimento di Scienze Fisiche dell'Università Federico II di Napoli, I-80125 Napoli, Italy

[u] INFN Sezione di Bari, I-70126 Bari, Italy

[v] INFN Sezione di Bologna, I-40127 Bologna, Italy

[w] Hamburg University, D-22761 Hamburg, Germany

[x] ITEP-Institute for Theoretical and Experimental Physics 317259 Moscow, Russia

[y] Toho University, J-274-8510 Funabashi, Japan

[z] Dipartimento di Fisica dell'Università di Padova, 35131 I-Padova, Italy

[aa] Department of Physics, Technion, IL-32000 Haifa, Israel

[ab] Università degli Studi di Urbino "Carlo Bo", I-61029 Urbino - Italy

[ac] INFN Sezione di Roma , I-00185 Roma, Italy

[ad] Nagoya University, J-464-8602 Nagoya, Japan

[ae] IRB-Rudjer Boskovic Institute, HR-10002 Zagreb, Croatia

[af] Gyeongsang National University, ROK-900 Gazwa-dong, Jinju 660-300, Korea

[ag] Aichi University of Education, J-448-8542 Kariya (Aichi-Ken), Japan

[ah] Dipartimento di Fisica dell'Università di Bari, I-70126 Bari, Italy

[ai] (MSU SINP) Lomonosov Moscow State University Skobeltsyn Institute of Nuclear Physics, RUS-119992 Moscow, Russia

[aj] Dipartimento di Fisica dell'Università di Roma Sapienza, I-00185 Roma, Italy

[ak] Utsunomiya University, J-321-8505 Utsunomiya, Japan

[al] IIHE, Université Libre de Bruxelles, B-1050 Brussels, Belgium

Abstract

The OPERA neutrino experiment at the underground Gran Sasso Laboratory has measured the velocity of neutrinos from the CERN CNGS beam over a baseline of about 730 km with much higher accuracy than previous studies conducted with accelerator neutrinos. The measurement is based on high-statistics data taken by OPERA in the years 2009, 2010 and 2011. Dedicated upgrades of the CNGS timing system and of the OPERA detector, as well as a high precision geodesy campaign for the measurement of the neutrino baseline, allowed reaching comparable systematic and statistical accuracies. An early arrival time of CNGS muon neutrinos with respect to the one computed assuming the speed of light in vacuum of $(60.7 \pm 6.9 \,(\text{stat.}) \pm 7.4 \,(\text{sys.}))$ ns was measured. This anomaly corresponds to a relative difference of the muon neutrino velocity with respect to the speed of light $(v\text{-}c)/c = (2.48 \pm 0.28 \,(\text{stat.}) \pm 0.30 \,(\text{sys.})) \times 10^{-5}$.

1. Introduction

The OPERA neutrino experiment [1] at the underground Gran Sasso Laboratory (LNGS) was designed to perform the first detection of neutrino oscillations in direct appearance mode in the $\nu_\mu \rightarrow \nu_\tau$ channel, the signature being the identification of the τ^- lepton created by its charged current (CC) interaction [2].

In addition to its main goal, the experiment is well suited to determine the neutrino velocity with high accuracy through the measurement of the time of flight and the distance between the source of the CNGS neutrino beam at CERN (CERN Neutrino beam to Gran Sasso) [3] and the OPERA detector at LNGS. For CNGS neutrino energies, $\langle E_\nu \rangle = 17$ GeV, the relative deviation from the speed of light c of the neutrino velocity due to its finite rest mass is expected to be smaller than 10^{-19}, even assuming the mass of the heaviest neutrino *eigenstate* to be as large as 2 eV [4]. Hence, a larger deviation of the neutrino velocity from c would be a striking result pointing to new physics in the neutrino sector. So far, no established deviation has been observed by any experiment.

In the past, a high energy ($E_\nu > 30$ GeV) and short baseline experiment has been able to test deviations down to $|v\text{-}c|/c < 4 \times 10^{-5}$ [5]. With a baseline analogous to that of OPERA but at lower neutrino energies (E_ν peaking at ~3 GeV with a tail extending above 100 GeV), the MINOS experiment reported a measurement of $(v\text{-}c)/c = 5.1 \pm 2.9 \times 10^{-5}$ [6]. At much lower energy, in the 10 MeV range, a stringent limit of $|v\text{-}c|/c < 2 \times 10^{-9}$ was set by the observation of (anti) neutrinos emitted by the SN1987A supernova [7].

In this paper we report on the precision determination of the neutrino velocity, defined as the ratio of the precisely measured distance from CERN to OPERA to the time of flight of neutrinos travelling through the Earth's crust. We used the high-statistics data taken by OPERA in the years 2009, 2010 and 2011. Dedicated upgrades of the timing systems for the time tagging of the CNGS beam at CERN and of the OPERA detector at LNGS resulted in a reduction of the systematic uncertainties down to the level of the statistical error. The measurement also relies on a high-accuracy geodesy campaign that allowed measuring the 730 km CNGS baseline with a precision of 20 cm.

2. The OPERA detector and the CNGS neutrino beam

The OPERA neutrino detector at LNGS is composed of two identical Super Modules, each consisting of an instrumented target section with a mass of about 625 tons followed by a magnetic muon spectrometer. Each section is a succession of walls filled with emulsion film/lead units interleaved with pairs of 6.7×6.7 m^2 planes of 256 horizontal and vertical scintillator strips composing the Target Tracker (TT). The TT allows the location of neutrino interactions in the target. This detector is also used to measure the arrival time of neutrinos. The scintillating strips are read out on both sides through WLS Kuraray Y11 fibres coupled to 64-channel Hamamatsu H7546 photomultipliers [8]. Extensive information on the OPERA experiment is given in [1] and in particular for the TT in [9].
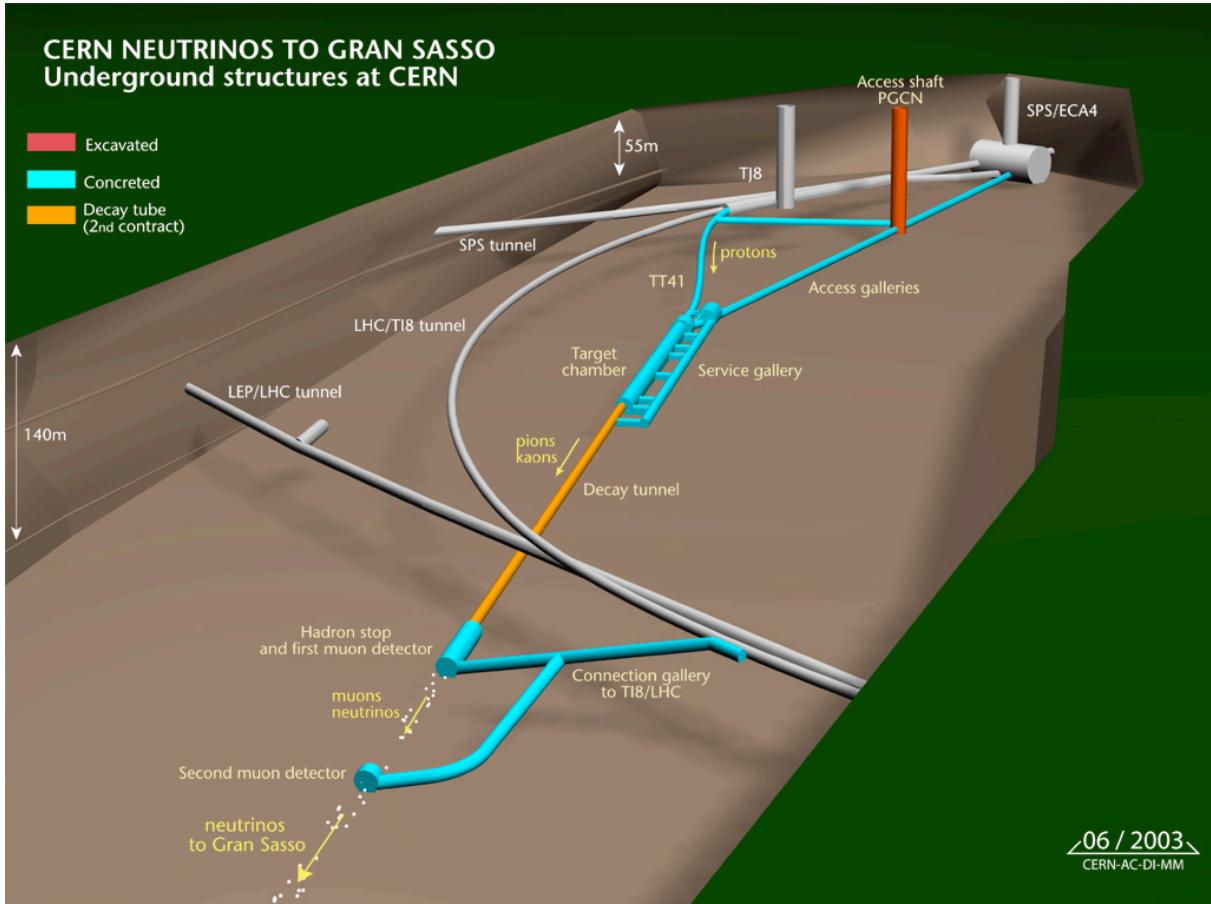

Fig. 1: Artistic view of the SPS/CNGS layout.

The CNGS beam is produced by accelerating protons to 400 GeV/c with the CERN Super Proton Synchrotron (SPS). These protons are ejected with a kicker magnet towards a 2 m long graphite neutrino production target in two extractions, each lasting 10.5 μs and separated by 50 ms. Each CNGS cycle in the SPS is 6 s long. Secondary charged mesons are focused by two magnetic horns, each followed by a helium bag to minimise the interaction probability of the

mesons. Mesons decay in flight into neutrinos in a 1000 m long vacuum tunnel. The SPS/CNGS layout is shown in Fig. 1. The different components of the CNGS beam are shown in Fig. 2.

The distance between the neutrino target and the OPERA detector is about 730 km. The CNGS beam is an almost pure ν_μ beam with an average energy of 17 GeV, optimised for $\nu_\mu \rightarrow \nu_\tau$ appearance oscillation studies. In terms of interactions in the detector, the $\bar{\nu}_\mu$ contamination is 2.1%, while ν_e and $\bar{\nu}_e$ contaminations are together smaller than 1%. The FWHM of the neutrino beam at the OPERA location is 2.8 km.
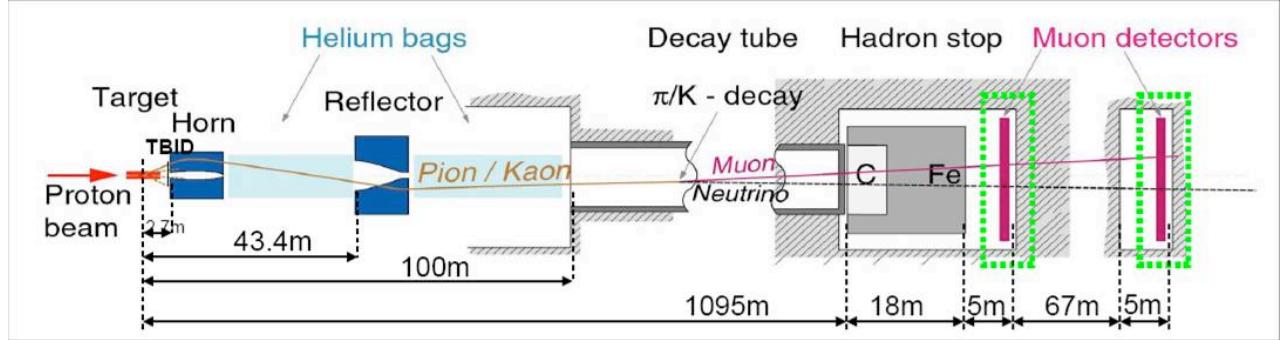
Fig.2: Layout of the CNGS beam line.

The kicker magnet trigger-signal for the proton extraction from the SPS is UTC (Coordinated Universal Time) time-stamped with a Symmetricom Xli GPS receiver [10]. The schematic of the SPS/CNGS timing system is shown in Fig. 3. The determination of the delays shown in Fig. 3 is described in Section 6.

The proton beam time-structure is accurately measured by a fast Beam Current Transformer (BCT) detector [11] (BFCTI400344) located (743.391 ± 0.002) m upstream of the centre of the graphite target and read out by a 1 GS/s Wave Form Digitizer (WFD) Acqiris DP110 [12]. The BCT consists of toroidal transformers coaxial to the proton beam providing a signal proportional to the beam current instantaneously transiting through it, with a few hundred MHz bandwidth. The start of the digitisation window of the WFD is triggered as well by the magnet kicker signal. The waveforms recorded for each extraction by the WFD are stamped with the UTC and stored in the CNGS database.

The proton beam has a coarse bunch structure corresponding to the 500 kHz of the CERN Proton Synchrotron (PS) (left part of Fig. 4), on which the fine structure due to the 200 MHz SPS radiofrequency is superimposed, which is actually resolved by the BCT measurement, as seen in the right part of Fig. 4.
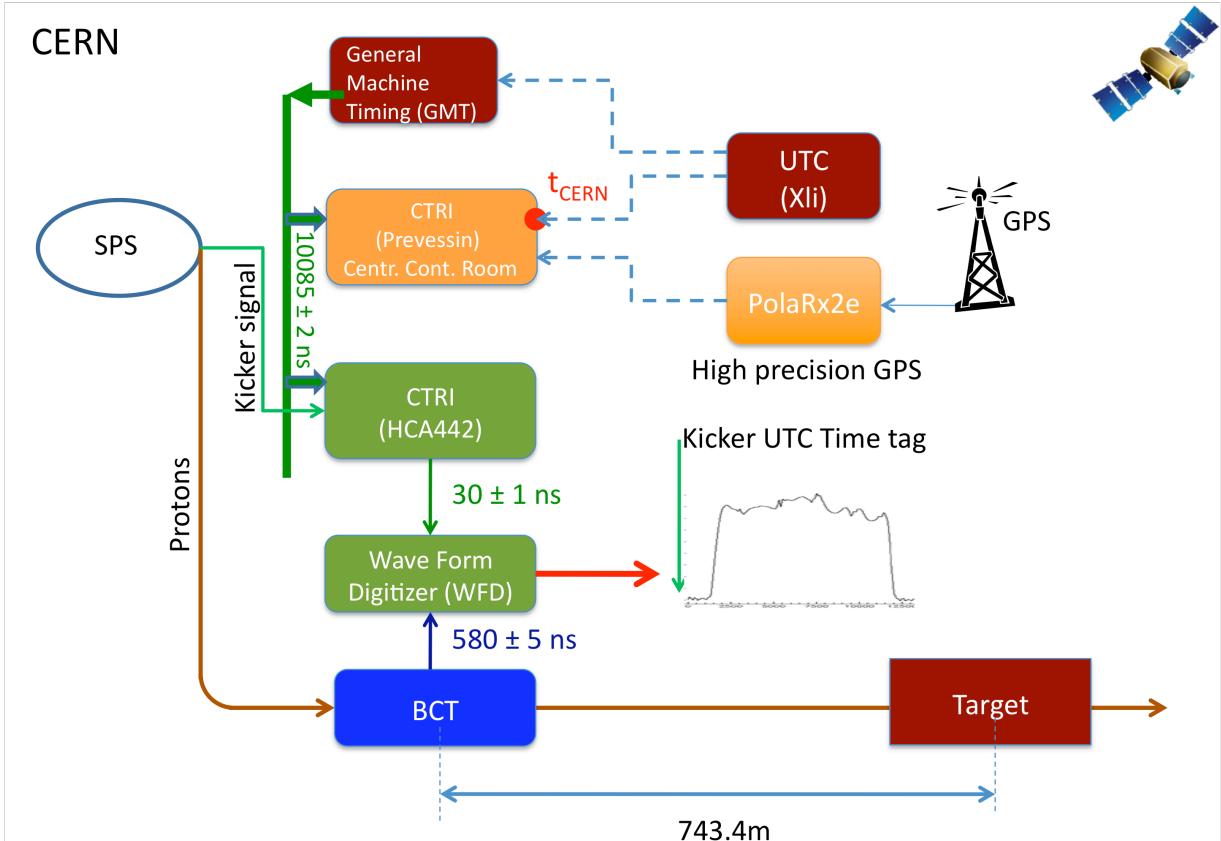
Fig. 3: Schematic of the CERN SPS/CNGS timing system. Green boxes indicate detector time-response. Orange boxes refer to elements of the CNGS-OPERA synchronisation system. Details on the various elements are given in Section 6.
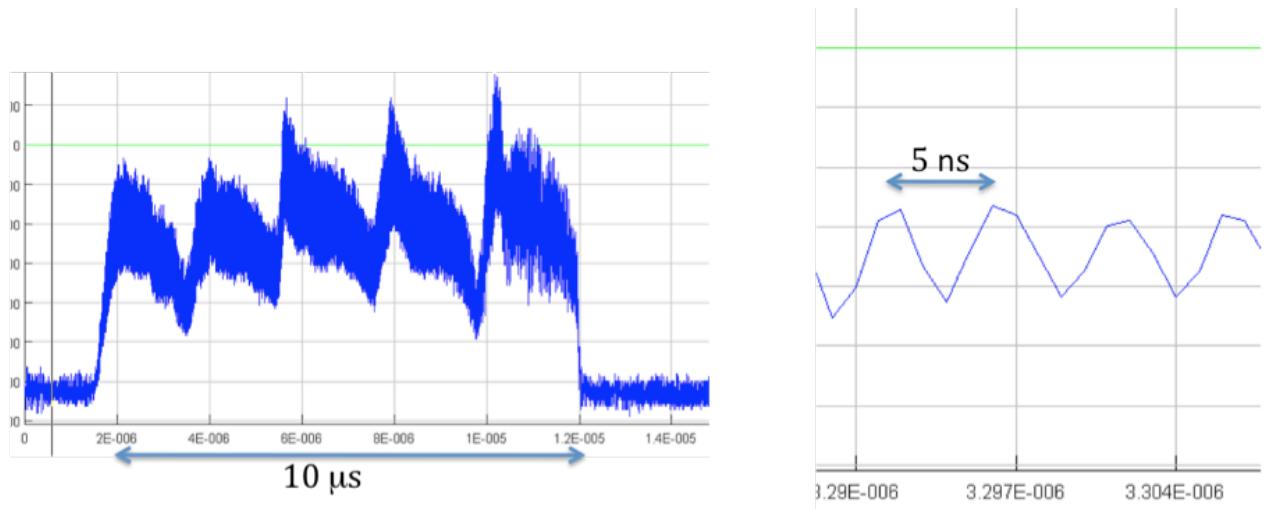

Fig. 4: Example of a proton extraction waveform measured with the BCT detector BFCTI400344. The five-peak structure reflects the continuous PS turn extraction mechanism. A zoom of the waveform (right plot) allows resolving the 200 MHz SPS radiofrequency.

3. Principle of the neutrino time of flight measurement

A schematic description of the principle of the time of flight measurement is shown in Fig. 5. The time of flight of CNGS neutrinos (TOF_ν) cannot be precisely measured at the single interaction level since any proton in the 10.5 μs extraction time may produce the neutrino detected by OPERA. However, by measuring the time distributions of protons for each extraction for which neutrino interactions are observed in the detector, and summing them together, after proper normalisation one obtains the probability density function (PDF) of the time of emission of the neutrinos within the duration of extraction. Each proton waveform is UTC time-stamped as well as the events detected by OPERA. The two time-stamps are related by TOF_c, the expected time of flight assuming the speed of light [13]. It is worth stressing that this measurement does not rely on the difference between a start (t_0) and a stop signal but on the comparison of two event time distributions.

The PDF distribution can then be compared with the time distribution of the interactions detected in OPERA, in order to measure TOF_ν. The deviation $\delta t = TOF_c - TOF_\nu$ is obtained by a maximum likelihood analysis of the time tags of the OPERA events with respect to the PDF, as a function of δt. The individual measurement of the waveforms reflecting the time structure of the extraction reduces systematic effects related to time variations of the beam compared to the case where the beam time structure is measured on average, *e.g.* by a near neutrino detector without using proton waveforms.
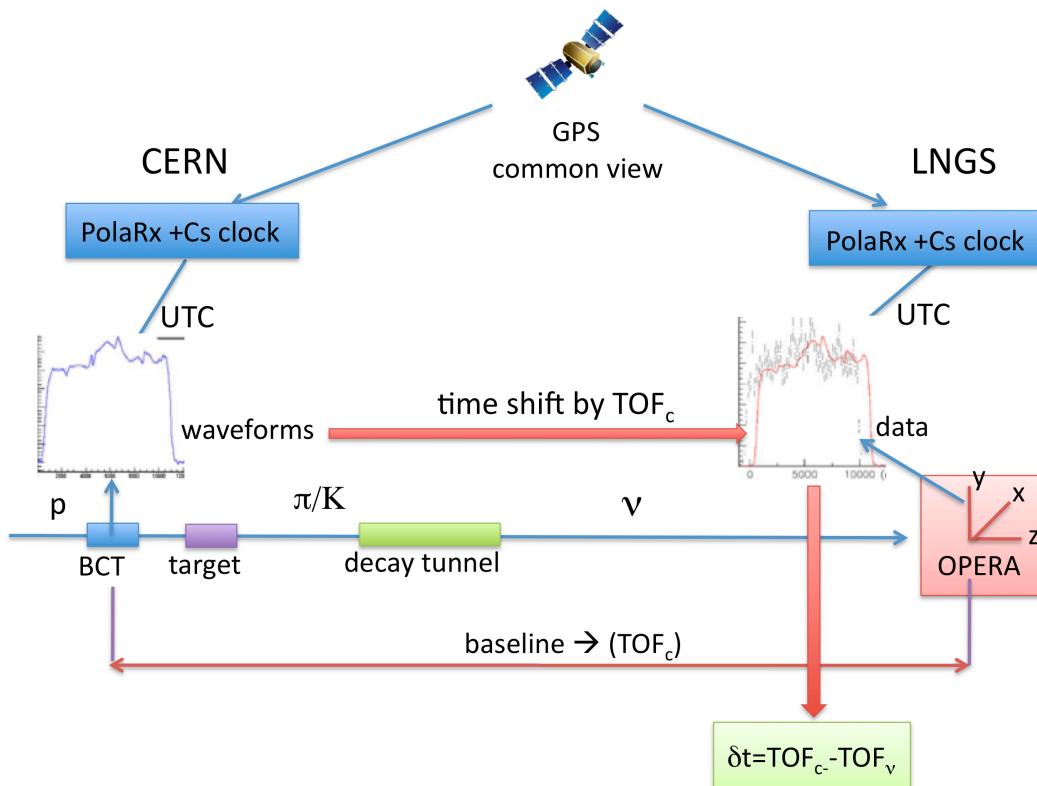

Fig. 5: Schematic of the time of flight measurement.

The total statistics used for the analysis reported in this paper is of 16111 events detected in OPERA, corresponding to about 10^{20} protons on target collected during the 2009, 2010 and 2011 CNGS runs. This allowed estimating δt with a small statistical uncertainty, presently comparable to the total systematic uncertainty.

The point where the parent meson produces a neutrino in the decay tunnel is unknown. However, this introduces a negligible inaccuracy in the neutrino time of flight measurement, because the produced mesons are also travelling with nearly the speed of light. By a full FLUKA based simulation of the CNGS beam [14] it was shown that the time difference computed assuming a particle moving at the speed of light from the neutrino production target down to LNGS, with respect to the value derived by taking into account the speed of the relativistic parent meson down to its decay point is less than 0.2 ns. Similar arguments apply to muons produced in muon neutrino CC interactions occurring in the rock in front of the OPERA detector and seen in the apparatus (external events). With a full GEANT simulation of external events it is shown that ignoring the position of the interaction point in the rock introduces a bias smaller than 2 ns with respect to those events occurring in the target (internal events), provided that external interactions are selected by requiring identified muons in OPERA. More details on the muon identification procedure are given in [15].
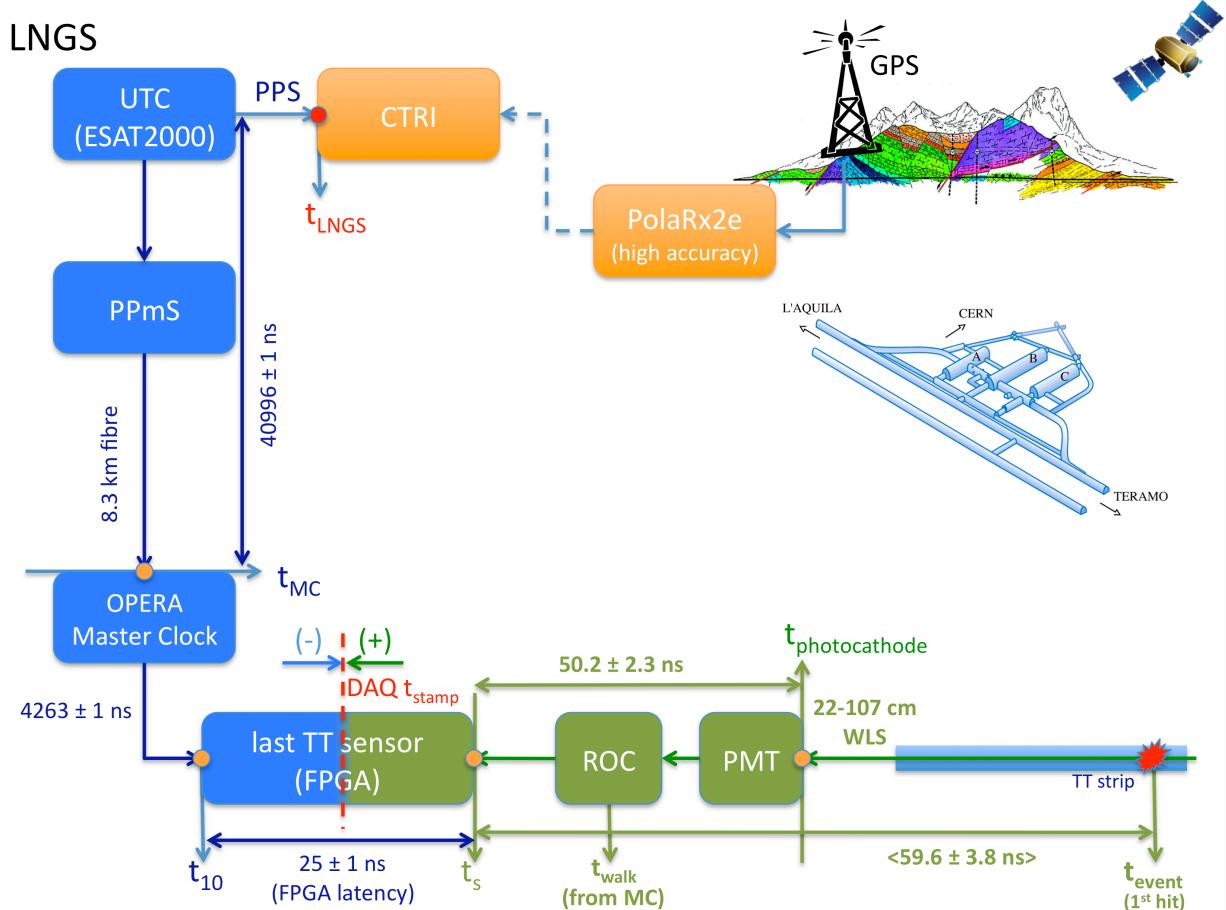

Fig. 6: Schematic of the OPERA timing system at LNGS. Blue delays include elements of the time-stamp distribution; increasing delays decrease the value of δt. Green delays indicate detector time-response; increasing delays increase the value of δt. Orange boxes refer to elements of the CNGS-OPERA synchronisation system.

A key feature of the neutrino velocity measurement is the accuracy of the relative time tagging at CERN and at the OPERA detector. The standard GPS receivers formerly installed at CERN and LNGS would feature an insufficient ~100 ns accuracy for the TOF_ν measurement. Thus, in 2008, two identical systems, composed of a GPS receiver for time-transfer applications Septentrio PolaRx2e [16] operating in "common-view" mode [17] and a Cs atomic clock Symmetricom Cs4000 [18], were installed at CERN and LNGS (see Figs. 3, 5 and 6).

The Cs4000 oscillator provides the reference frequency to the PolaRx2e receiver, which is able to time-tag its "One Pulse Per Second" output (1PPS) with respect to the individual GPS satellite observations. The latter are processed offline by using the CGGTTS format [19]. The two systems feature a technology commonly used for high-accuracy time transfer applications [20]. They were calibrated by the Swiss Metrology Institute (METAS) [21] and established a permanent time link between two reference points (t_{CERN} and t_{LNGS}) of the timing chains of CERN and OPERA at the nanosecond level. This time link between CERN and OPERA was independently verified by the German Metrology Institute PTB (Physikalisch-Technische Bundesanstalt) [22] by taking data at CERN and LNGS with a portable time-transfer device [23]. The difference between the time base of the CERN and OPERA PolaRx2e receivers was measured to be (2.3 ± 0.9) ns [22]. This correction was taken into account in the application of the time link.

All the other elements of the timing distribution chains of CERN and OPERA were accurately calibrated by using different techniques, further described in the following, in order to reach a comparable level of accuracy.

4. Measurement of the neutrino baseline

The other fundamental ingredient for the neutrino velocity measurement is the knowledge of the distance between the point where the proton time-structure is measured at CERN and the origin of the underground OPERA detector reference frame at LNGS. The relative positions of the elements of the CNGS beam line are known with millimetre accuracy. When these coordinates are transformed into the global geodesy reference frame ETRF2000 [24] by relating them to external GPS benchmarks, they are known within 2 cm accuracy.

The analysis of the GPS benchmark positions was first done by extrapolating measurements taken at different periods via geodynamical models [25], and then by comparing simultaneous measurements taken in the same reference frame. The two methods yielded the same result within 2 cm [26]. The travel path of protons from the BCT to the focal point of the CNGS target is also known with millimetre accuracy.

The distance between the target focal point and the OPERA reference frame was precisely measured in 2010 following a dedicated geodesy campaign. The coordinates of the origin of the OPERA reference frame were measured by establishing GPS benchmarks at the two sides of the ~10 km long Gran Sasso highway tunnel and by transporting their positions with a terrestrial traverse down to the OPERA detector. A common analysis in the ETRF2000 reference frame of the 3D coordinates of the OPERA origin and of the target focal point allowed the determination

of this distance to be (730534.61 ± 0.20) m [26]. The 20 cm uncertainty is dominated by the long underground link between the outdoors GPS benchmarks and the benchmark at the OPERA detector [26].

The high-accuracy time-transfer GPS receiver allows to continuously monitor tiny movements of the Earth's crust, such as continental drift that shows up as a smooth variation of less than 1 cm/year, and the detection of slightly larger effects due to earthquakes. The April 2009 earthquake in the region of LNGS, in particular, produced a sudden displacement of about 7 cm, as seen in Fig. 7. All mentioned effects are within the accuracy of the baseline determination. Tidal effects are negligible as well.

The baseline considered for the measurement of the neutrino velocity is then the sum of the (730534.61 ± 0.20) m between the CNGS target focal point and the origin of the OPERA detector reference frame, and the (743.391 ± 0.002) m between the BCT and the focal point, *i.e.* (731278.0 ± 0.2) m.
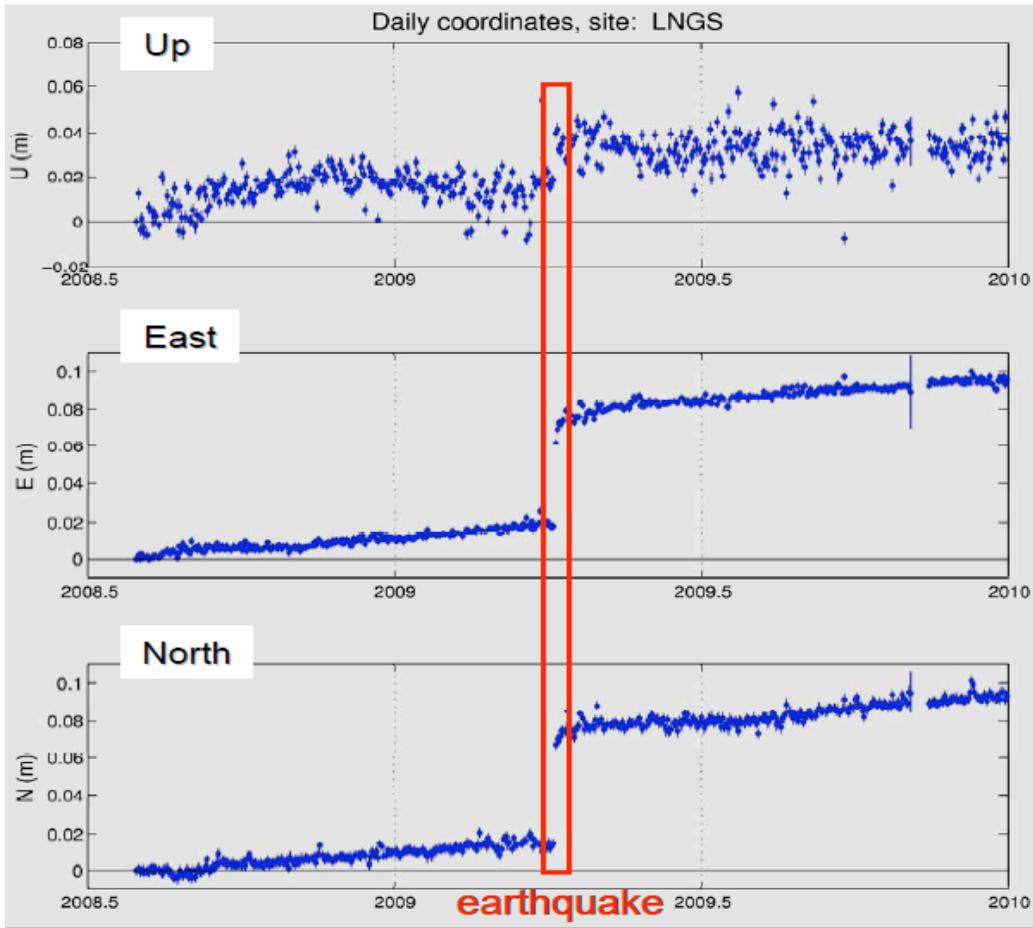

Fig. 7: Monitoring of the PolaRx2e GPS antenna position at LNGS, showing the slow earth crust drift and the fault displacement due to the 2009 earthquake in the L'Aquila region. Units for the horizontal (vertical) axis are years (meters).

10

5. Data selection

The OPERA data acquisition system (DAQ) time-tags the detector TT hits with 10 ns quantization with respect to the UTC [27]. The time of a neutrino interaction is defined as that of the earliest hit in the TT. CNGS events are preselected by requiring that they fall within a window of $\pm$ 20 μs with respect to the SPS kicker magnet trigger-signal, delayed by the neutrino time of flight assuming the speed of light and corrected for the various delays of the timing systems at CERN and OPERA. The relative fraction of cosmic-ray events accidentally falling in this window is 10^{-4}, and it is therefore negligible [1, 28].

Since TOF_c is computed with respect to the origin of the OPERA reference frame, located beneath the most upstream spectrometer magnet, the time of the earliest hit for each event is corrected for its distance along the beam line from this point, assuming a time propagation according to the speed of light. The UTC time of each event is also individually corrected for the instantaneous value of the time link correlating the CERN and OPERA timing systems.

The total statistics used for this analysis consists of 7586 internal (charged and neutral current interactions) and 8525 external (charged current) events. Internal events, preselected by the electronic detectors with the same procedure used for neutrino oscillation studies [29], constitute a subsample of the entire OPERA statistics (about 70%) for which both time transfer systems at CERN and LNGS were operational, as well as the database-logging of the proton waveforms. As mentioned before, external events, in addition, are requested to have a muon identified in the detector.

6. Neutrino event timing

The schematic of the SPS/CNGS timing system is shown in Fig. 3. A general-purpose timing receiver "Control Timing Receiver" (CTRI) at CERN [30] logs every second the difference in time between the 1PPS outputs of the Xli and of the more precise PolaRx2e GPS receivers, with 0.1 ns resolution. The Xli 1PPS output represents the reference point of the time link to OPERA. This point is also the source of the "General Machine Timing" chain (GMT) serving the CERN accelerator complex [31].

The GPS devices are located in the CERN Prevessin Central Control Room (CCR). The time information is transmitted via the GMT to a remote CTRI device in Hall HCA442 (former UA2 experiment counting room) used to UTC time-stamp the kicker magnet signal. This CTRI also produces a delayed replica of the kicker magnet signal, which is sent to the adjacent WFD module. The UTC time-stamp marks the start of the digitization window of the BCT signal. The latter signal is brought via a coaxial cable to the WFD at a distance of 100 m. Three delays characterise the CERN timing chain:

a) The propagation delay through the GMT of the time base of the CTRI module logging the PolaRx2e 1PPS output to the CTRI module used to time-tag the kicker pulse $\Delta t_{UTC} = (10085 \pm 2)$ ns;

b) The delay to produce the replica of the kicker magnet signal from the CTRI to start the WFD $\Delta t_{trigger} = (30 \pm 1)$ ns;

c) The delay from the time the protons cross the BCT to the time a signal arrives to the WFD $\Delta t_{BCT} = (580 \pm 5)$ ns.

The kicker signal is just used as a pre-trigger and as an arbitrary time origin. The measurement of the TOF_v is based instead on the BCT waveforms, which are tagged with respect to the UTC.

The measurement of Δt_{UTC} was performed by means of a portable Cs4000 oscillator. Its 1PPS output, stable to better than 1ns over a few hour scale, was input to the CTRI used to log the Xli 1PPs signal at the CERN CCR. The same signal was then input to the CTRI that time-stamps the kicker signal at the HCA442 location. The two measurements allowed the determination of the delay between the time bases of the two CTRI, and to relate the kicker time-stamp to the Xli output. The measurements were repeated three times during the last two years and yielded the same results within 2 ns. This delay was also determined by performing a two-way timing measurement with optical fibres. The Cs clock and the two-way measurements also agree within 2 ns.

The two-way measurement is a technique used several times in this analysis for the determination of delays. Measuring the delay t_A in propagating a signal to a far device consists in sending the same signal via an optical fibre B to the far device location in parallel to its direct path A. At this site the time difference t_A-t_B between the signals following the two paths is measured. A second measurement is performed by taking the signal arriving at the far location via its direct path A and sending it back to the origin with the optical fibre B. At the origin the time difference between the production and receiving time of the signal corresponds to t_A+t_B. In this procedure the optoelectronic chain used for the fibre transmission of the two measurements is kept identical by simply swapping the receiver and the transmitter between the two locations. The two combined measurements allow determining t_A and t_B [32].

$\Delta t_{trigger}$ was estimated by an accurate oscilloscope measurement. The determination of Δt_{BCT} was first performed by measuring the 1PPS output of the Cs4000 oscillator with a digital oscilloscope and comparing to a CTRI signal at the point where the BCT signal arrives at the WFD. This was compared to similar measurement where the Cs4000 1PPS signal was injected into the calibration input of the BCT. The time difference of the 1PPS signals in the two configurations led to the measurement of $\Delta t_{BCT} = (581 \pm 10)$ ns.

Since the above determination through the calibration input of the BCT might not be representative of the internal delay of the BCT with respect to the transit of the protons, a more sophisticated method was then applied. The proton transit time was tagged upstream of the BCT by two fast beam pick-ups BPK400099 and BPK400207 with a time response of ~1 ns [33]. From the relative positions of the three detectors (the pick-ups and the BCT) along the beam line and the signals from the two pick-ups one determines the time the protons cross the BCT and the time delay at the level of the WFD. In order to achieve an accurate determination of the delay between the BCT and the BPK signals, a measurement was performed in the particularly clean experimental condition of the SPS proton injection to the Large Hadron Collider (LHC) machine

of 12 bunches with 50 ns spacing, passing through the BCT and the two pick-up detectors. This measurement was performed simultaneously for the 12 bunches and yielded Δt_{BCT} = (580 ± 5 (sys.)) ns.

The schematic of the OPERA timing system at LNGS is shown in Fig. 6. The official UTC time source at LNGS is provided by a GPS system ESAT 2000 [34, 35] operating at the surface laboratory. The 1PPS output of the ESAT is logged with a CTRI module every second with respect to the 1PPS of the PolaRx2e, in order to establish a high-accuracy time link with CERN. Every millisecond a pulse synchronously derived from the 1PPS of the ESAT (PPmS) is transmitted to the underground laboratory via an 8.3 km long optical fibre. The delay of this transmission with respect to the ESAT 1PPS output down to the OPERA master clock output was measured with a two-way fibre procedure and amounts to (40996 ± 1) ns. Measurements with a transportable Cs clock were also performed yielding the same result. The OPERA master clock is disciplined by a high-stability oscillator Vectron OC-050 with an Allan deviation of 2×10^{-12}/s. This oscillator keeps the local time in between two external synchronisations given by the PPmS signals coming from the external GPS.

The time base of the OPERA master clock is transmitted to the frontend cards of the TT. This delay (Δt_{clock}) was also measured with two techniques, namely by the two-way fibres method and by transporting the Cs4000 clock to the two points. Both measurements provided the same result of (4263 ± 1) ns. The frontend card time-stamp is performed in a FPGA (Field Programmable Gate Arrays) by incrementing a coarse counter every 0.6 s and a fine counter with a frequency of 100 MHz. At the occurrence of a trigger the content of the two counters provides a measure of the arrival time. The fine counter is reset every 0.6 s by the arrival of the master clock signal that also increments the coarse counter. The internal delay of the FPGA processing the master clock signal to reset the fine counter was determined by a parallel measurement of trigger and clock signals with the DAQ and a digital oscilloscope. The measured delay amounts to (24.5 ± 1.0) ns. This takes into account the 10 ns quantization effect due to the clock period.

The delays in producing the Target Tracker signal including the scintillator response, the propagation of the signals in the WLS fibres, the transit time of the photomultiplier [8], and the time response of the OPERA analogue frontend readout chip (ROC) [36] were overall calibrated by exciting the scintillator strips at known positions by a UV picosecond laser [37]. The arrival time distribution of the photons to the photocathode and the time walk due to the discriminator threshold in the analogue frontend chip as a function of the signal pulse height were accurately parameterized in laboratory measurements and included in the detector simulation. The total time elapsed from the moment photons reach the photocathode, a trigger is issued by the ROC analogue frontend chip, and the trigger arrives at the FPGA, where it is time-stamped, was determined to be (50.2 ± 2.3) ns.

Since the time response to neutrino interactions depends on the position of the hits in the detector and on their pulse height, the average TT delay was evaluated by computing the difference between the exact interaction time and the time-stamp of the earliest hit for a sample of fully simulated neutrino interactions. Starting from the position at which photons are generated in each strip, the simulation takes into account all the effects parametrized from laboratory measurements including the arrival time distribution of the photons for a given production

position, the time-walk of the ROC chip, and the measured delays from the photocathode to the FPGA. This TT delay has an average value of 59.6 ns with a RMS of 7.3 ns, reflecting the transverse event distribution inside the detector. The 59.6 ns represent the overall delay of the TT response down to the FPGA and they include the above-mentioned delay of 50.2 ns. A systematic error of 3 ns was estimated due to the simulation procedure.

Several checks were performed by comparing data and simulated events, as far as the earliest TT hit timing is concerned. Data and simulations agree within the Monte Carlo systematic uncertainty of 3 ns for both the time difference between the earliest and the following hits, and for the difference between the earliest hit and the average hit timing of muon tracks.

More details on the neutrino timing as well as on the geodesy measurement procedures can be found in [38].

7. Data analysis

The data analysis was performed blindly by deliberately assuming the setup configuration of 2006. In particular, important calibrations were not available at all that time, such as the BCT delay Δt_{BCT}, the trigger delay $\Delta t_{trigger}$ and the improved estimate of the UTC delay Δt_{UTC}. Also TOF_c was not expressed with respect to the BCT position but referred to another conventional point upstream in the beam line. DAQ and detector delays were not taken into account either. This led by construction to an unrealistically large deviation from TOF_c, much larger than the individual calibration contributions. The precisely calibrated corrections applied to TOF_v and yielding the final δt value are summarized in Table 1.

For each neutrino interaction measured in the OPERA detector the analysis procedure used the corresponding proton extraction waveform. These were summed up and properly normalised in order to build a PDF w(t). The WFD is triggered by the magnet kicker pulse, but the time of the proton pulses with respect to the kicker trigger is different for the two extractions. The kicker trigger is just related to the pulsing of the kicker magnet. The exact timing of the proton pulses stays within this large window of the pulse.

A separate maximum likelihood procedure was then carried out for the two proton extractions. The likelihood function to be maximised for each extraction is a function of the single variable δt to be added to the time tags t_j of the OPERA events. These are expressed in the time reference of the proton waveform digitizer assuming neutrinos travelling at the speed of light, such that their distribution best coincides with the corresponding PDF:

$$L_k\left(\delta t_k\right)=\prod_j w_k\left(t_j+\delta t_k\right) \quad \text{k=1,2 extractions}$$

Near the maximum the likelihood function can be approximated by a Gaussian function, whose variance is a measure of the statistical uncertainty on δt (Fig. 8). As seen in Fig. 9, the PDF representing the time-structure of the proton extraction is not flat but exhibits a series of peaks and valleys, reflecting the features and the inefficiencies of the proton extraction from the

PS to the SPS via the Continuous Turn mechanism [39]. Such structures may well change with time. The way the PDF are built automatically accounts for the beam conditions corresponding to the neutrino interactions detected by OPERA. The result of the maximum likelihood analysis of δt for the two proton extractions for the years 2009, 2010 and 2011 are compared in Fig. 10. They are compatible with each other.

Table 1: Summary of the time delay values used in the blind analysis and those corresponding to the final analysis.

	Blind 2006	Final analysis	Correction (ns)
Baseline (ns)	2440079.6	2439280.9	
Correction baseline			-798.7
CNGS DELAYS :			
UTC calibration (ns)	10092.2	10085	
Correction UTC			-7.2
WFD (ns)	0	30	
Correction WFD			30
BCT (ns)	0	-580	
Correction BCT			-580
OPERA DELAYS :			
TT response (ns)	0	59.6	
FPGA (ns)	0	-24.5	
DAQ clock (ns)	-4245.2	-4262.9	
Correction TT+FPGA+DAQ			17.4
GPS syncronization (ns)	-353	0	
Time-link (ns)	0	-2.3	
Correction GPS			350.7
Total			-987.8

Data were also grouped in arbitrary subsamples to look for possible systematic dependences. For example, by computing δt separately for events taken during day and night hours, the absolute difference between the two bins is (17.1 ± 15.5) ns providing no indication for a systematic effect. A similar result was obtained for a possible summer vs spring + fall dependence, which yielded (11.3 ± 14.5) ns.

The maximum likelihood procedure was checked with a Monte Carlo simulation. Starting from the experimental PDF, an ensemble of 100 data sets of OPERA neutrino interactions was simulated. Simulated data were shifted in time by a constant quantity, hence faking a time of flight deviation. Each sample underwent the same maximum likelihood procedure as applied to real data. The analysis yielded a result accounting for the statistical fluctuations of the sample that are reflected in the different central values and their uncertainties. The average of the central values from this ensemble of simulated OPERA experiments reproduces well the time shift applied to the simulation (at the 0.3 ns level). The average statistical error extracted from the likelihood analysis also reproduces within 1 ns the RMS distribution of the mean values with respect to the true values.
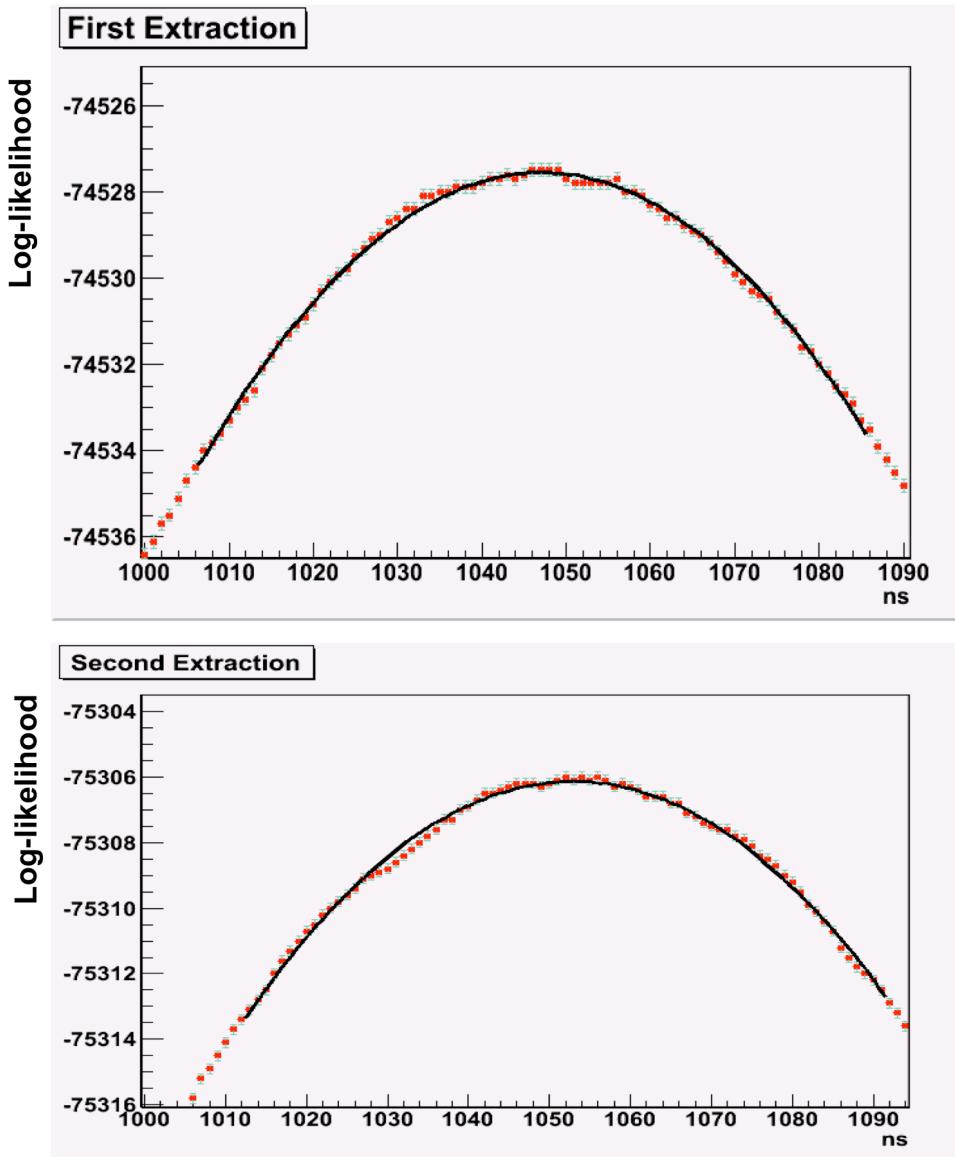
Fig. 8: Log-likelihood distributions for both extractions as a function of δt, shown close to the maximum and fitted with a parabolic shape for the determination of the central value and of its uncertainty.

The result of the blind analysis shows an earlier arrival time of the neutrino with respect to the one computed by assuming the speed of light δt (blind) = TOF_c -TOF_v = (1048.5 ± 6.9 (stat.)) ns. As a check, the same analysis was repeated considering only internal events. The result is δt (blind) = (1047.4 ± 11.2 (stat.)) ns, compatible with the systematic error of 2 ns due to the inclusion of external events. The agreement between the proton PDF and the neutrino time distribution obtained after shifting by δt (blind) is illustrated in Fig. 11. The $χ^2$/ndf is 1.06 for the first extraction and 1.12 for the second one. Fig. 12 shows a zoom of the leading and trailing edges of the distributions given in the bottom of Fig. 11.
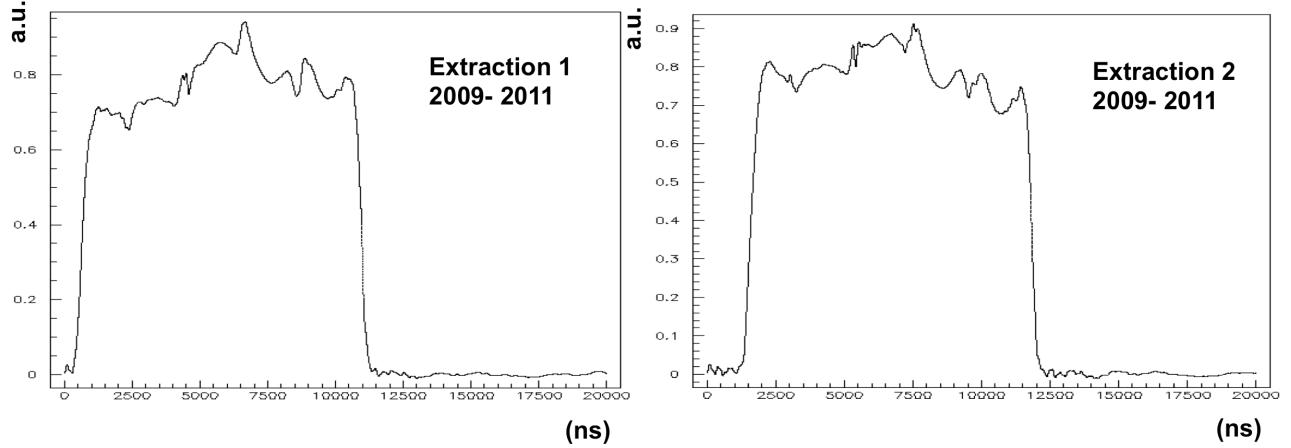
Fig. 9: Summed proton waveforms of the OPERA events corresponding to the two SPS extractions for the 2009, 2010 and 2011 data samples.
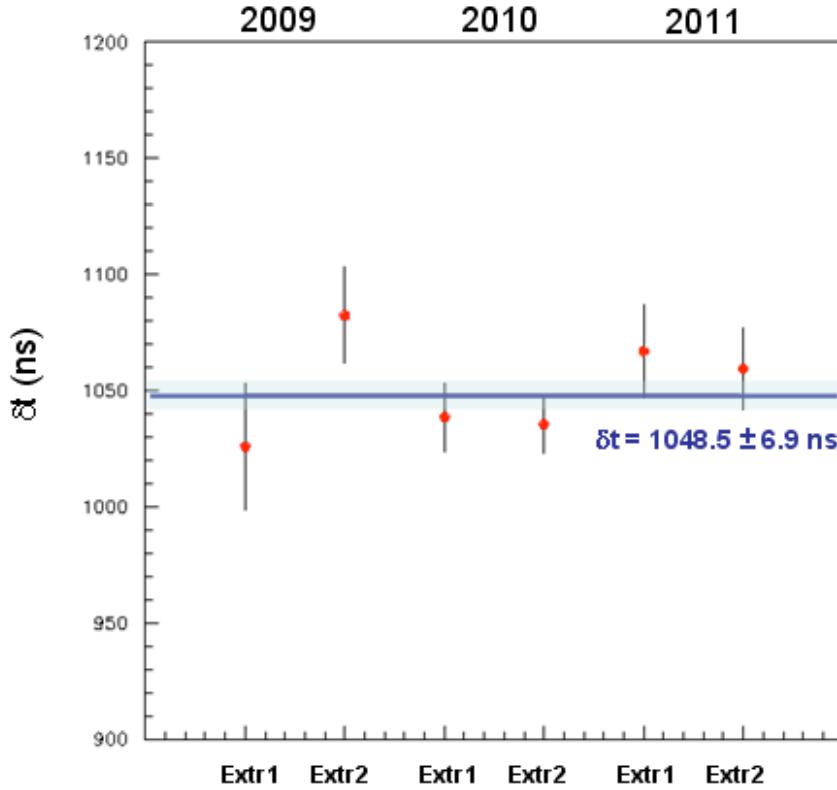
Fig. 10: Results of the maximum likelihood analysis for δt corresponding to the two SPS extractions for the 2009, 2010 and 2011 data samples.

The blind analysis lasted until all elements of the distance measurement and the timing chains had been accurately calibrated. The box was then opened including all corrections of the distance measurement and the timing chains. The corrections applied to the UTC time-stamps used in the blind analysis and after the precise calibration of all these values are summarised in Table 1. In order to ease the interpretation of the corrections a sign is attributed to each

17

calibration value. The delays that increase (decrease) the value of δt = TOF_c - TOF_v have a positive (negative) sign. Each correction is computed as the difference between the value corresponding to the final analysis and the one assumed in the blind analysis.
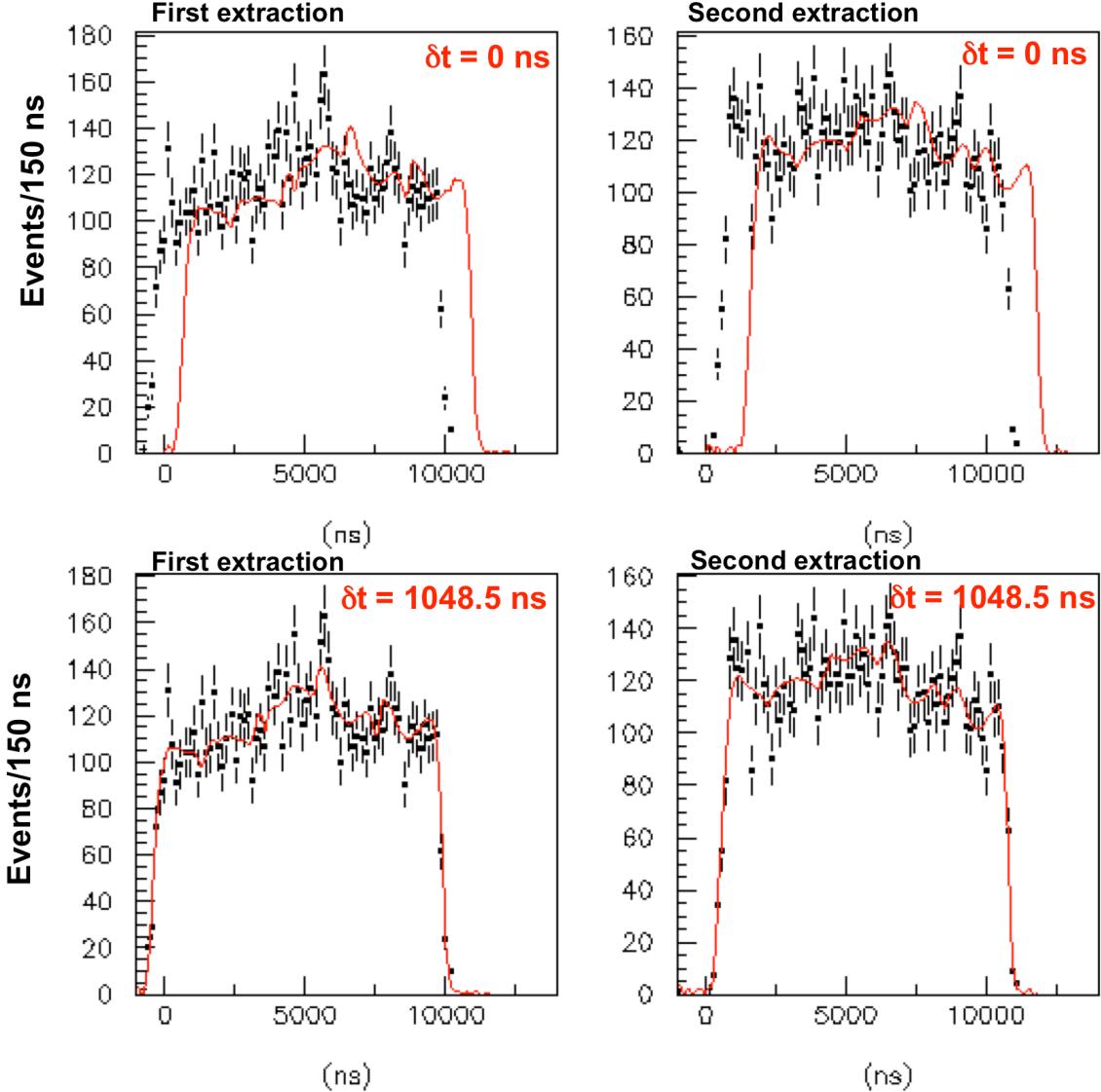
Fig. 11: Comparison of the measured neutrino interaction time distributions (data points) and the proton PDF (red line) for the two SPS extractions before (top) and after (bottom) correcting for δt (blind) resulting from the maximum likelihood analysis.

The 17.4 ns correction in Table 1 takes into account all the effects related to DAQ and TT delays, as well as the difference between the value of Δt_{clock} determined in 2006 from a test-bench measurement and the one obtained on-site with the procedure previously described. The 353 ns relative to the 2006 calibration assume the relative synchronisation of the CERN and LNGS GPS systems prior to the installation of the two high-accuracy systems operating in common-view mode. One then obtains:

$$\delta t = TOF_c - TOF_v = 1048.5 \ ns - 987.8 \ ns = (60.7 \pm 6.9 \ (stat.)) \ ns$$

The above result is also affected by an overall systematic uncertainty of 7.4 ns coming from the quadratic sum of the different terms previously discussed in the text and summarised in Table 2. The dominant contribution is due to the calibration of the BCT time response. The error in the CNGS-OPERA GPS synchronisation has been computed by adding in quadrature the uncertainties on the calibration performed by the PTB and the internal uncertainties of the two high-accuracy GPS systems. The final result of the measurement is (Fig. 13):

$$\delta t = TOF_c - TOF_\nu = (60.7 \pm 6.9 \text{ (stat.)} \pm 7.4 \text{ (sys.))} \text{ ns.}$$

We cannot explain the observed effect in terms of presently known systematic uncertainties. Therefore, the measurement indicates an early arrival time of CNGS muon neutrinos with respect to the one computed assuming the speed of light in vacuum. The relative difference of the muon neutrino velocity with respect to the speed of light is:

$$(v\text{-}c)/c = \delta t /(TOF'_c - \delta t) = (2.48 \pm 0.28 \text{ (stat.)} \pm 0.30 \text{ (sys.))} \times 10^{-5},$$

with 6.0 σ significance. In performing this last calculation a baseline of 730.085 km was used, and TOF'_c corresponds to this effective neutrino baseline starting from the average decay point in the CNGS tunnel as determined by simulations. Actually, the δt value is measured over the distance from the BCT to the OPERA reference frame, and it is only determined by neutrinos and not by protons and pions, which introduce negligible delays.
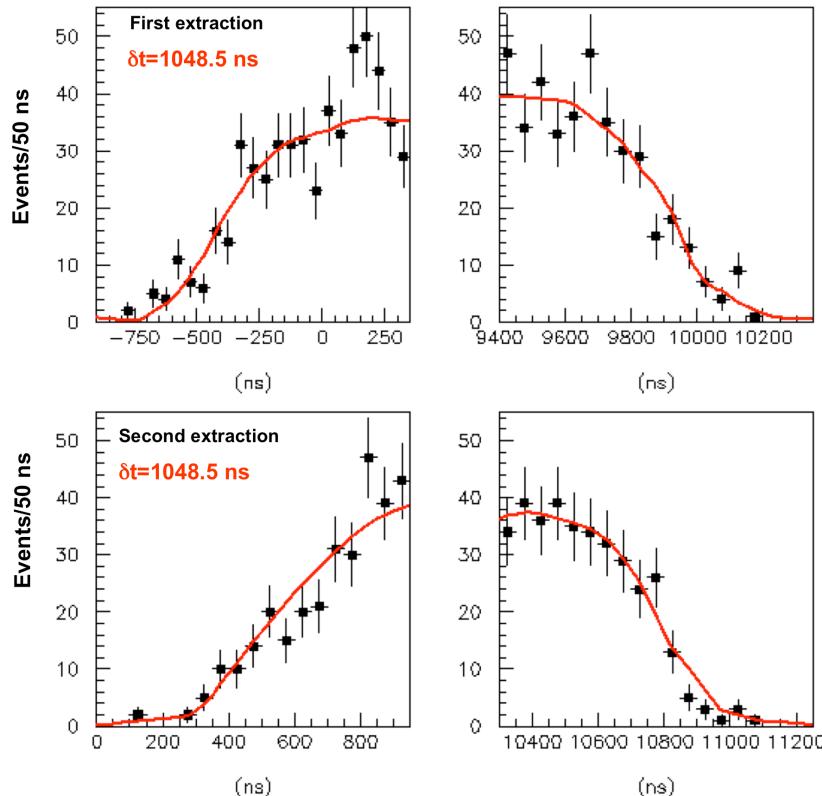

Fig. 12: Zoom of the leading (left plots) and trailing edges (right plots) of the measured neutrino interaction time distributions (data points) and the proton PDF (red line) for the two SPS extractions after correcting for δt (blind).

Table 2: Contribution to the overall systematic uncertainty on the measurement of δt.

Systematic uncertainties	ns
Baseline (20 cm)	0.67
Decay point	0.2
Interaction point	2.0
UTC delay	2.0
LNGS fibres	1.0
DAQ clock transmission	1.0
FPGA calibration	1.0
FWD trigger delay	1
CNGS-OPERA GPS synchronisation	1.7
MC simulation for TT timing	3.0
TT time response	2.3
BCT calibration	5.0
Total sys. uncertainty (in quadrature)	**7.4**

A possible neutrino energy dependence of δt was studied in order to investigate the physics origin of the early arrival time of CNGS neutrinos. For this analysis the data set was limited to ν_μ CC interactions occurring in the OPERA target (5489 events), for which the neutrino energy can be measured by adding the muon momentum to the hadronic energy. Details on the energy reconstruction in the OPERA detector are available in [15]. A first measurement was performed by considering all ν_μ CC internal events. We obtained δt = (60.3 ± 13.1 (stat.) ± 7.4 (sys.)) ns, for an average neutrino energy of 28.1 GeV.

Data were then split into two bins of nearly equal statistics, including events of energy lower or higher than 20 GeV. The mean energies of the two samples are 13.9 and 42.9 GeV. The result for the low- and high-energy data sets are, respectively, δt = (53.1 ± 18.8 (stat.) ± 7.4 (sys.)) ns and (67.1 ± 18.2 (stat.) ± 7.4 (sys.)) ns. The above result was checked against a full Monte Carlo simulation of the OPERA events. The same procedure used for real data was applied to ν_μ CC simulated interactions in the OPERA target. The comparison between the two data sets indicates no energy dependence, with a difference of ~1 ns. The simulation does not indicate any instrumental effects on δt possibly caused by an energy dependent time response of the detector. Therefore, the systematic uncertainties of the two measurements tend to cancel each other out regarding the difference of the two values, which amounts to (14.0 ± 26.2) ns. This result, illustrated in Fig. 13, provides no clues on a possible energy dependence of δt in the domain explored by OPERA, within the statistical accuracy of the measurement.
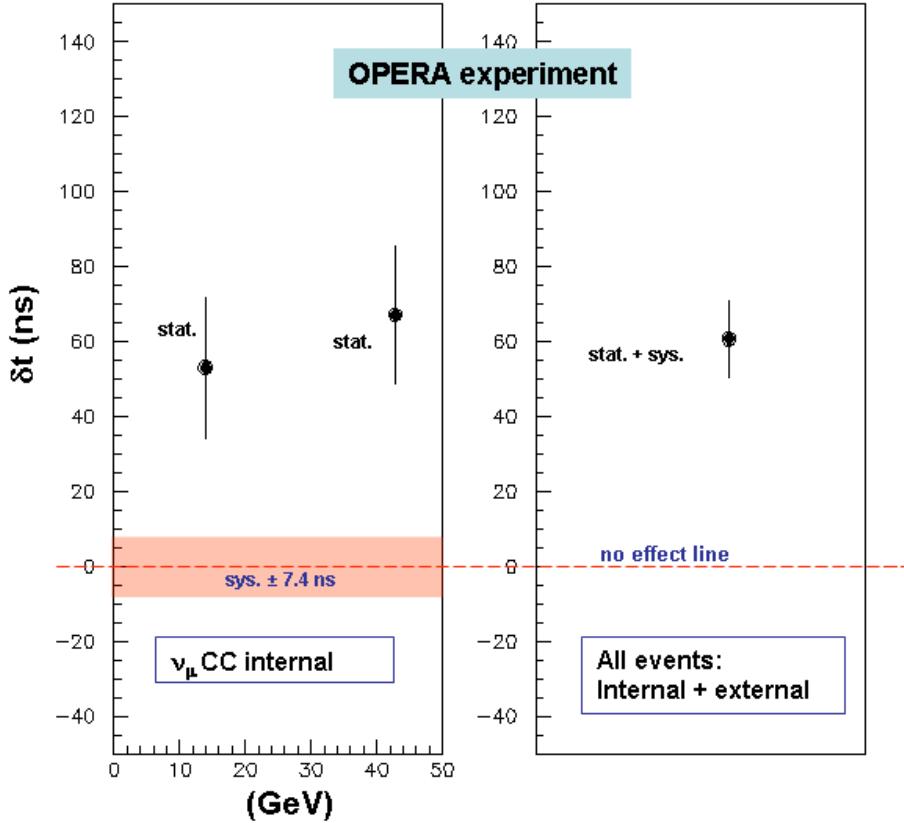
Fig. 13: Summary of the results for the measurement of δt. The left plot shows δt as a function of the energy for ν_μ CC internal events. The errors attributed to the two points are just statistical in order to make their relative comparison easier since the systematic error (represented by a band around the no-effect line) cancels out. The right plot shows the global result of the analysis including both internal and external events (for the latter the energy cannot be measured). The error bar includes statistical and systematic uncertainties added in quadrature.

Conclusions

The OPERA detector at LNGS, designed for the study of neutrino oscillations in appearance mode, has provided a precision measurement of the neutrino velocity over the 730 km baseline of the CNGS neutrino beam sent from CERN to LNGS through the Earth's crust. A time of flight measurement with small systematic uncertainties was made possible by a series of accurate metrology techniques. The data analysis took also advantage of a large sample of about 16000 neutrino interaction events detected by OPERA.

The analysis of internal neutral current and charged current events, and external ν_μ CC interactions from the 2009, 2010 and 2011 CNGS data was carried out to measure the neutrino velocity. The sensitivity of the measurement of (v-c)/c is about one order of magnitude better than previous accelerator neutrino experiments.

The results of the study indicate for CNGS muon neutrinos with an average energy of 17 GeV an early neutrino arrival time with respect to the one computed by assuming the speed of light in vacuum:

$$\delta t = (60.7 \pm 6.9 \text{ (stat.)} \pm 7.4 \text{ (sys.)}) \text{ ns.}$$

The corresponding relative difference of the muon neutrino velocity and the speed of light is:

$$(v\text{-}c)/c = \delta t / (\text{TOF'}_c - \delta t) = (2.48 \pm 0.28 \text{ (stat.)} \pm 0.30 \text{ (sys.)}) \times 10^{-5}.$$

with an overall significance of 6.0 σ.

The dependence of δt on the neutrino energy was also investigated. For this analysis the data set was limited to the 5489 ν_μ CC interactions occurring in the OPERA target. A measurement performed by considering all ν_μ CC internal events yielded $\delta t = (60.3 \pm 13.1 \text{ (stat.)} \pm 7.4 \text{ (sys.)}) \text{ ns}$, for an average neutrino energy of 28.1 GeV. The sample was then split into two bins of nearly equal statistics, taking events of energy higher or lower than 20 GeV. The results for the low- and high-energy samples are, respectively, $\delta t = (53.1 \pm 18.8 \text{ (stat.)}) \pm 7.4 \text{ (sys.)}) \text{ ns}$ and $(67.1 \pm 18.2 \text{ (stat.)}) \pm 7.4 \text{ (sys.)}) \text{ ns}$. This provides no clues on a possible energy dependence of δt in the domain explored by OPERA within the accuracy of the measurement.

Despite the large significance of the measurement reported here and the stability of the analysis, the potentially great impact of the result motivates the continuation of our studies in order to investigate possible still unknown systematic effects that could explain the observed anomaly. We deliberately do not attempt any theoretical or phenomenological interpretation of the results.

References

[1] OPERA Collaboration, R. Acquafredda et al., JINST 4 (2009) P04018.

[2] A. Ereditato, K. Niwa and P. Strolin, The emulsion technique for short, medium and long baseline $v_\mu \rightarrow v_\tau$ oscillation experiments, 423, INFN-AE-97-06, DAPNU-97-07;

OPERA collaboration, H. Shibuya et al., Letter of intent: the OPERA emulsion detector for a long-baseline neutrino-oscillation experiment, CERN-SPSC-97-24, LNGS-LOI-8-97;

OPERA collaboration, M. Guler et al., An appearance experiment to search for $v_\mu \rightarrow v_\tau$ oscillations in the CNGS beam: experimental proposal, CERN-SPSC-2000-028, LNGS P25/2000;

OPERA collaboration, M. Guler et al., Status Report on the OPERA experiment, CERN/SPSC 2001-025, LNGS-EXP 30/2001 add. 1/01;

OPERA Collaboration, N. Agafonova et al., Phys. Lett. B 691 (2010) 138;

OPERA Collaboration, N. Agafonova et al., arXiv:1107.2594v1.

[3] Ed. K. Elsener, The CERN Neutrino beam to Gran Sasso (Conceptual Technical Design), CERN 98-02, INFN/AE-98/05;

R. Bailey et al., The CERN Neutrino beam to Gran Sasso (NGS) (Addendum to CERN 98-02, INFN/AE-98/05), CERN-SL/99-034(DI), INFN/AE-99/05.

[4] Ch. Weinheimer et al., Phys. Lett. B 460 (1999) 219;

Ch. Weinheimer et al., Phys. Lett. B 464 (1999) 352;

M. Lobashev et al., Phys. Lett. B 460 (1999) 227.

[5] G. R. Kalbfleisch , Phys. Rev. Lett. 43, 1361 (1979);

J. Alspector et al., Phys. Rev. Lett. 36, 837 (1976).

[6] MINOS Collaboration, P. Adamson at al., Phys. Rev. D 76 (2007) 072005.

[7] K. Hirata et al., Phys. Rev. Lett. 58 (1987) 1490;

R. M. Bionta et al., Phys. Rev. Lett. 58 (1987) 1494;

M. J. Longo, Phys. Rev. D 36 (1987) 3276.

[8] Hamamatsu Photonics K.K., Electron Tube Center, 314-5, Shimokanzo, Toyooka-village, Iwata-gun, Shizuoka-ken 438–0193, Japan.

[9] T. Adam et al., Nucl. Instr. and Meth. A 577 (2007) 523.

[10] http://www.symmetricom.com/products/gps-solutions/gps-time-frequency-receivers/XLi/.

[11] H. Jacob et al., CERN-AB 2003-056 BDI.

[12] Agilent Acqiris digitizer model DP110: http://www.agilent.com -> Technical support -> Manuals -> Part number U1607A.

[13] K. Nakamura et al. (Particle Data Group), J. Phys. G 37, 075021 (2010).

[14] FLUKA software package: http://www.fluka.org; CNGS neutrino flux calculations:

http://www.mi.infn.it/~psala/Icarus/cngs.html ; G. Battistoni et al., AIP Conference Proceedings, 896m (2007) 31.

[15] OPERA Collaboration, N. Agafanova et al., New J. Phys. 13 (2011) 053051.

[16] P. Defraigne et al., Initial testing of a new GPS receiver, the PolaRx2e, for time and frequency transfer using dual frequency codes and carrier phases, in: 35th Annual Precise Time and Time Interval (PTTI) Meeting.

[17] D. W. Allan and M. A. Weiss, Accurate time and frequency transfer during common-view of a GPS satellite, in: Proc. 34th Ann. Freq. Control Symposium, USAERADCOM, Ft. Monmouth, WJ 07703, May 1980.

[18] Symmetricon frequency standards, Symmetricom, Time and Frequency System.

http://www.symmetricom.com/products/frequency-references/cesium-frequency-standard/Cs4000/.

[19] D. Allan and C. Thomas, Technical Directives for Standardization of GPS Time Receiver Software to be implemented for improving the accuracy of GPS common-view time transfer, Metrologia 31, 1994;
J. Asoubin and W. Lewandowksi, CGGTTS GPS/GLONASS Data Format V02, BIPM November 1998.

[20] P. Defraigne and G. Petit, Time Transfer to TAI Using Geodetic Receivers, Metrologia, 40, 184 (2003);
J. Levine, A review of Time and Frequency Transfer Methods, Metrologia, 45, 184 (2008).

[21] METAS Measurement Reports No 119-00210, No 119-00209: Differential calibration of matched GPS receiver, antenna and cable against reference GPS link METAS WAB2 CH01 for P3 common-view time transfer.

[22] Physikalisch-Technische Bundesanstalt (PTB), http://www.ptb.de; Relative calibration of the GPS time link between CERN and LNGS, Report calibration CERN-LNGS 2011.

[23] T. Feldmann et al., Advanced GPS-based time link calibration with PTB's new GPS calibration setup, 42nd Annual Precise Time and Time Interval (PTTI) Meeting.

[24] IERS, http://www.iers.org/nn_11216/IERS/EN/IERSHome/home.html;
C. Boucher and Z. Altamimi, Memo: Specifications for reference frame fixing in the analysis of a EUREF GPS campaign, http://etrs89.ensg.ign.fr/memo-V7.pdf.

[25] EUREF Permanent Network, http://www.epncb.oma.be/.

[26] G. Colosimo, M. Crespi, A. Mazzoni, M. Jones and D. Missiaen, "Determination of the CNGS global geodesy", OPERA public note 132 (2011).

[27] J. Marteau for the OPERA Collaboration, Nucl. Instr. and Meth. A 617 (2010) 291.

[28] OPERA Collaboration, R. Acquafredda, et al., New J. Phys. 8 (2006) 303.

[29] A. Bertolin and N. T. Tran, OpCarac: an algorithm for the classification of the neutrino interactions recorded by OPERA, OPERA public note 100 (2009); http://operaweb.lngs.infn.it:2080/Opera/publicnotes/note100.pdf.

[30] P. Alvarez, The CTR user guide, 17 July 2007, CERN EDMS document of the beam timing group;
J. Serrano et al., Nanosecond level UTC timing generation and stamping in the CERN's LHC, proceedings of ICALEPCS2003, 119 (2003).

[31] J. Lewis et al., The evolution of the CERN SPS timing system for the LHC era, proceedings of ICALEPCS2003, 125 (2003).

[32] J.Serrano et al., Inter-laboratory synchronisation for the CNGS project, proceedings of EPAC2006, 3092 (2006).

[33] L. Jensen, Beam Instrumentation for the CNGS facility, AB-Note-2006-022 BI.

[34] Master clock GPS 2000, http://www.esat.it/EN/default.htm, M. Ambrosio, et al., Phys. Rev. D 62 (2000) 052003.

[35] M.Ambrosio et al., The MACRO detector at Gran Sasso, Nucl. Instr. and Meth. in Physics Research A 486 (2002) 663.

[36] A. Lucotte et al., Nucl. Instr. and Meth. A 521 (2004) 378392.

[37] A.L.S. GmbH ; The Picosecond Laser Diode Systems, http://www.alsgmbh.com/pilas.htm.

[38] Neutrino velocity measurement with the OPERA experiment in the CNGS beams, G. Brunetti, PhD thesis, in joint supervision from Université Claude Bernard Lyon-I and Università di Bologna, 2011.

[39] M. Giovannozzi et al., The CERN PS multi-turn extraction based on beam splitting in stable islands of transverse phase space: Design Report, CERN-2006-011.